Electrical Power and Energy Systems 98 (2018) 488–495

Contents lists available at ScienceDirect

Electrical Power and Energy Systems

journal homepage: www.elsevier.com/locate/ijepes

Linear synthetic inertia for improved frequency quality and reduced hydropower wear and tear

Linn Saarinen[1], Per Norrlund[2], Weijia Yang[3], Urban Lundin*

Division of Electricity, Department of Engineering Sciences, Uppsala University, SE-751 21 Uppsala, Sweden

ARTICLE INFO

Keywords:
Synthetic inertia
Hydropower
Frequency control
Virtual synchronous machine
Wear and tear

ABSTRACT

The power system inertia is decreasing in many electrical grids as the share of production from directly connected synchronous generators decreases. Lower inertia increases the frequency deviations in normal operation, which leads to increased wear and tear in hydropower turbines and other units providing frequency control to the system. The predominant concepts for synthetic inertia from for example wind power does not address the frequency quality in normal operation, only the acute problem of frequency stability during large disturbances. This paper investigates how the frequency quality and frequency controlling hydropower units are affected by decreasing inertia and damping, using the Nordic power system as a case study. A new type of synthetic inertia (SI), which is linear and continuously active, is suggested as a means to mitigate the impacts on these units. It is shown that the suggested linear SI controller can effectively replace synchronous inertia and damping, improving frequency quality and reducing hydropower wear and tear. The controller includes an energy recovery feedback loop, to avoid depletion of the energy source behind the controller. The power and energy needed to provide linear SI is quantified, and the impact of the SI energy recovery integration time constant is investigated.

1. Introduction

The electricity production from variable renewable energy (VRE) sources is increasing all over the world. In addition to having a weather dependent power output, these production units are normally connected to the grid through inverters, which means that they do not supply the grid with natural inertia like synchronous machines do. As VRE is replacing production from synchronous machines, the inertia of the power system decreases and the number of units that can provide frequency containment reserves, FCR (also called primary control) and frequency restoration reserves, FRR (also called secondary control), without curtailment decreases. In the European Union, this development has prompted the transmission system operators (TSOs) to include obligations for large generators to provide FCR and some type of inertia in the draft of the new grid code [1,2]. Hydro-Québec in Canada and EirGrid in Ireland have already specified requirements on inertia emulation from wind farms in their grid codes [3,4].

Decreasing inertia can have an impact on several aspects of grid stability [5]. The aspect that has drawn most attention so far is the impact on the rate of change of frequency (ROCOF) and the lowest frequency (the nadir) after a sudden disconnection of the largest unit in the system (the n − 1 disturbance). Early grid code requirements on synthetic inertia (SI), like the ones by Hydro-Québec [3] and EirGrid [4], are clearly focusing on this aspect, and commercial implementations of SI, such as GE's WindINERTIA [6] and ENERCON's IE [7] are designed to support the grid only during large frequency events.

Another aspect is the frequency quality during normal operation. Reduced inertia increases the amplitude and frequency of the grid frequency variations [8]. This changes the operational pattern of FCR, leading to more regulation and increased wear and tear of the units delivering frequency control reserves to the grid, for example hydropower [9,10], which may lead to increasing costs for frequency control. It also affects the worst case nadir for an n − 1 disturbance, since the frequency may already be low when the disturbance occurs. The impact on normal operation has been overlooked in studies on synthetic inertia so far.

A third aspect is that reduced inertia and damping may impact the modes of electro-mechanical oscillations in the system. The conventional way to address electro-mechanical oscillations is to use power system stabilizers (PSSs) on synchronous generators. As an alternative,

* Corresponding author.
E-mail address: urban.lundin@angstrom.uu.se (U. Lundin).
[1] Vattenfall Hydropower AB, Uppsalavägen 3, SE-814 70 Älvkarleby, Sweden.
[2] Vattenfall Research and Development, Älvkarlebylaboratoriet, SE-814 26 Älvkarleby, Sweden.
[3] State Key Laboratory of Water Resources and Hydropower Engineering Science, Wuhan University, Wuhan 430072, China.

https://doi.org/10.1016/j.ijepes.2017.12.007
Received 15 June 2017; Received in revised form 27 October 2017; Accepted 11 December 2017

both synthetic damping [11] and specialized controllers using notch filters [12] have been suggested for systems with a high share of VRE.

A wide range of solutions to the problem of decreasing inertia has been investigated. One end of the spectrum is virtual synchronous machines/generator (VISMA, VSM, VSG) [13–16] or synchronverters [17], that aim at creating an interface between the VRE and the grid that totally emulates a synchronous machine with inertia, damping, voltage control, etc., which is continuously active. The other end of the spectrum is emulated inertia as defined by for example Hydro-Québec, i.e. a fixed power output for a certain time period, that is triggered by large frequency events but otherwise inactive. The terms synthetic/emulated/virtual inertia tend to be used for the types of grid support that are only active during large disturbances. They can be either fixed power profile [3,18] proportional to the grid frequency deviation (P-controller) [19] or proportional to the derivative of the grid frequency deviation (D-controller) [20,21]. Mathematically, D-control corresponds to inertia and P-control corresponds to damping, frequency dependent load or super fast droop control.

Synthetic inertia can be delivered by various sources, for example flywheels, superconducting magnetic energy storages [22], capacitors [23,24], batteries [13] or wind turbines [19,2]. In the case of wind turbines, it is the actual inertia of the unit that is the power source of the synthetic inertia, possibly in combination with extra power extracted from the wind, which is available if the wind speed is higher than the rated wind speed or if some power is being curtailed to create a margin for increase. The inertia can also be used to smooth the output power of the unit [25]. To maintain production efficiency, the wind turbine must be returned to its optimal rotational speed and pitch as soon as possible. This is one reason why research on SI from wind power is oriented towards temporary grid support during large disturbances, while continuously active VSM research normally assumes a large battery as the energy source. However, as long as the energy source is not inexhaustible, some type of energy recovery scheme will be needed. Such schemes has not yet been discussed in research on VSM.

This paper presents a new, linear SI controller which is continuously active, automatically recovers the energy of its energy source and can emulate both inertia and damping. The impact from reduced inertia and damping on the system during normal operation is described, and compared to a scenario where the lost inertia and damping are replaced with active control by the suggested linear SI controller. Furthermore, the impact of the energy recovery time constant of the SI is investigated, both in terms of linear and non-linear (limit cycle) aspects. Energy recovery schemes have previously been studied for temporarily active SI, but not for any of the continuously active concepts like VSM. To the best of our knowledge, the consequences for units delivering frequency control services to the system have not been previously been studied in relation to SI or VSM.

2. Method

In this paper, the Nordic synchronous grid is used as a case study. The system is dominated by hydro and nuclear power, and almost all FCR is delivered by hydropower. Onshore and offshore wind power is growing, at the same time as some nuclear power is scheduled for decommissioning. The organisation for European TSO:s, Entso-e, estimates that in 2020 the kinetic energy of the Nordic system during low load and high wind will be 124 GWs, which is only half of today's normal value, and as low as 80 GWs in 2025 [26]. It is also expected that the frequency dependency of the load will continue to decrease, as more and more loads are connected to the grid via inverters. The Nordic system is sensitive to changes in inertia and damping since the FCR is provided by hydropower with non-minimum phase response. There are already concerns about a very low frequency oscillation in the system [27]. This paper will compare normal operation in today's system with two scenarios: (1) System inertia and damping reduced by half and possibly replaced by synthetic reserves that are triggered at major frequency events, meaning that there is no support in normal operation, and (2) System inertia and damping reduced by half but replaced by continuously active synthetic reserves provided by the suggested linear SI controller, supporting normal operation. Both synthetic inertia (D-control) and synthetic damping (P-control) are investigated in this paper. For simplicity, the controller that provides these two types of grid support will be denoted SI-controller, and which type of service it provides is specified case by case.

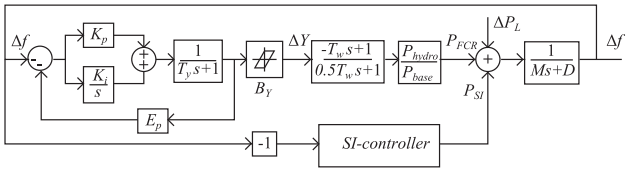

Fig. 1. One-area model of the Nordic synchronous system, where FCR is delivered by hydropower. The signal Δf is the grid frequency deviation, ΔY is the guide vane opening deviation, P_{FCR} is the FCR power output, P_{SI} is the power output from the SI controller and ΔP_L is the load disturbance. Parameter values are given in Table 1, where K_p,K_i and E_p are the governor parameters, T_y is the servo time constant, $\pm B_Y$ is the backlash in the guide vane regulating mechanism, T_w is the water time constant, M is the system inertia constant and D is the frequency dependency of the load (the system damping).

2.1. System

Since this study is focused on the impact on frequency control in normal operation, the power system can be modelled as a one-area model according to Fig. 1, with parameters according to Table 1, c.f. [27]. All the hydropower units delivering FCR are lumped into one unit, governed by a PI controller with droop. Backlash in the guide vane regulating mechanism after the feedback measurement of the guide vane position is included in the model. Measurements on Swedish hydropower units have shown that this type of backlash greatly impacts the performance of the FCR delivered in normal operation [28]. In the Entso-e scenario for 2020, the Nordic hydropower production in the low inertia scenario is 14.5 GW. If the hydropower is assumed to operate at 80% loading (typical best efficiency point), this means that the installed hydropower in operation, P_{hydro}, is 18 GW. Normally, the TSO:s in the Nordic system acquire a total FCR power $P_{FCR} = 7530$ MW/Hz FCR from the power producers. This corresponds to a per unit droop

$$E_p = \frac{1}{P_{FCR}} \frac{P_{hydro}}{f_{base}} = 0.048 \quad (1)$$

in the lumped model. The governor proportional and integral gain K_p and K_i are scaled with the droop E_p so that the dynamic response of the governor is the same as in the previously published model of today's system [27].

2.2. Linear SI controller

A block diagram of the suggested linear SI controller is drawn in Fig. 2. This is the top-level controller, and it is assumed that the delay of the actuation of the requested power output from the SI controller, P_{SI}, is fast enough to be negligible. This is reasonable if the energy source is

Table 1
System parameters in per unit with $P_{base} = 50$ GW. Low load case with total production 29 GW. $P_{hydro} = 20$ GW, cf. Fig. 1.

Scenario	M	D	T_w	B_Y	T_y	E_p	K_p	K_i
Nominal	14.6	0.57	1.01	0.001	0.2	0.048	4.2	0.38
$M = 0.5M_{nom}$	7.3	0.57	1.01	0.001	0.2	0.048	4.2	0.38
$D = 0.5D_{nom}$	14.6	0.285	1.01	0.001	0.2	0.048	4.2	0.38
Both	7.3	0.285	1.01	0.001	0.2	0.048	4.2	0.38

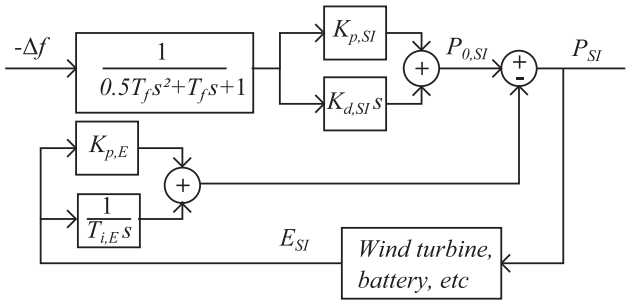

Fig. 2. The suggested linear SI controller. A PD-controller with a second order filter on the input signal (upper part) and an energy recovery feedback loop with a PI controller, that restores the energy of the source (i.e. the battery charging level, the rotational speed of the wind turbine, etc.).

controlled by an inverter which is faster than the low pass filter implemented in the controller. The upper part of the block diagram is a PD-controller (proportional-derivative), where the derivative part, $K_{d,SI}$ emulates inertia and the proportional part, $K_{p,SI}$, emulates damping. The correspondence between the system inertia, M, and $K_{d,SI}$ and the system damping, D, and $K_{p,SI}$ respectively can be derived by analysis of a simplified system without FCR and with the low pass filter and energy recovery loop of the SI controller neglected. The frequency deviation can then be expressed as

$$\Delta f = \frac{1}{Ms + D}(\Delta P_L - (K_{p,SI} + K_{d,SI}s)\Delta f), \tag{2}$$

which can be written as

$$\Delta f = \frac{1}{(M + K_{d,SI})s + D + K_{p,SI}}\Delta P_L. \tag{3}$$

To replace the lost inertia in the $M = M_{nom}/2$ case, $K_{d,SI}$ should therefore be set to

$$K_{d,SI} = M_{nom} - M = 7.3 \text{ pu}, \tag{4}$$

and, correspondingly, to replace damping in the $D = D_{nom}/2$ case, $K_{p,SI}$ should be set to

$$K_{p,SI} = D_{nom} - D = 0.285 \text{ pu}. \tag{5}$$

The input signal, frequency deviation Δf, is filtered with a second order low pass filter with time constant $T_f = 0.1$ s. A second order filter is required to achieve sufficient high frequency disturbance rejection in a derivative controller [29]. The power requested by the PD-controller is drawn from some type of energy reservoir, which could be capacitors, batteries, flywheels or the rotational energy of wind turbines. The most generic model of this reservoir is an integration, $1/s$, and the output signal is the total energy withdrawn from the reservoir. This energy, E_{SI}, has to be restored. If efficiency is lost due to the withdrawal of energy, like in the case of a wind turbine that is slowed down from its optimal speed, more energy has to be returned than what was withdrawn. A PI-controller (proportional-integrating) will restore the withdrawn energy E_{SI} to zero, and the speed of the recovery is determined by the proportional gain and the integration time constant of the recovery loop, $K_{p,E}$ and $T_{i,E}$.

There are many ways to tune a PI controller, and some of the classical methods like Ziegler-Nichols often give poor results. In this paper, a frequency domain tuning method is applied to tune the energy recovery loop. From the block diagram in Fig. 2, the power output from the SI controller can be expressed as

$$\Delta P_{SI} = \Delta P_{SI,0} - \frac{1}{s}\left(K_{p,E} + \frac{1}{T_{i,E}s}\right)\Delta P_{SI} \tag{6}$$

which can be simplified to

Table 2
Parameters of the SI energy recovery feedback loop, with different speed of the recovery.

Recovery scheme	C_0	C_1	C_2	C_3
$T_{i,E}$	∞	300,000 s	3000 s	30 s
$K_{p,E}$	0	0.01 pu	0.03 pu	0.26 pu

$$\Delta P_{SI} = \frac{s^2}{s^2 + K_{p,E}s + 1/T_{i,E}}\Delta P_{SI,0} \equiv S(s)\Delta P_{SI,0}. \tag{7}$$

A suitable requirement is that there is no overshoot in the response of the energy recovery loop, i.e. that P_0 is not amplified by $S(s)$. This requirement can be expressed in frequency domain as

$$\|S(i\omega)\|_\infty = \left\| \frac{(i\omega)^2}{(i\omega)^2 + K_{p,E}i\omega + 1/T_{i,E}} \right\|_\infty \leqslant 1. \tag{8}$$

The parameter $T_{i,E}$ can be selected freely depending on the size of the energy reservoir of the SI controller, and the parameter $K_{p,E}$ is selected to satisfy the equality in Eq. (8).

The SI controller parameters thus selected are given in Table 2. The step responses (open loop from f to P_{SI} and E_{SI}) of SI-controllers with varying energy recovery time are plotted in Fig. 3, where the controller delivers only inertia, and in Fig. 4, where the controller delivers only damping. Here, the input signal is a step in the input grid frequency of −0.01 pu.

2.3. Measures of frequency quality and control work

The impact on system performance will be quantified by three measures in this paper. The first is the grid frequency root mean square error. This measure of grid frequency quality describes the typical amplitude of the frequency deviations, but not their frequency. The Bode diagram is a good complement, since it also reveals if the system has low damping in some frequency bands.

The second measure is the travelled distance per hour of the guide vane regulating mechanism, Y_{dist}, in a typical hydropower unit providing FCR. The Y_{dist} is a measure of the wear of the turbine, since it is related to the sliding distance of the guide vane bearings and, in the case of a Kaplan turbine, the sliding distance of the runner bearings [30].

The third measure is the number of load cycles per hour of the guide vane regulating mechanism, Y_{cycles}, in a typical hydropower unit providing FCR. The number of load cycles is defined as half the number of direction changes of the guide vane opening signal. The Y_{cycles} is a

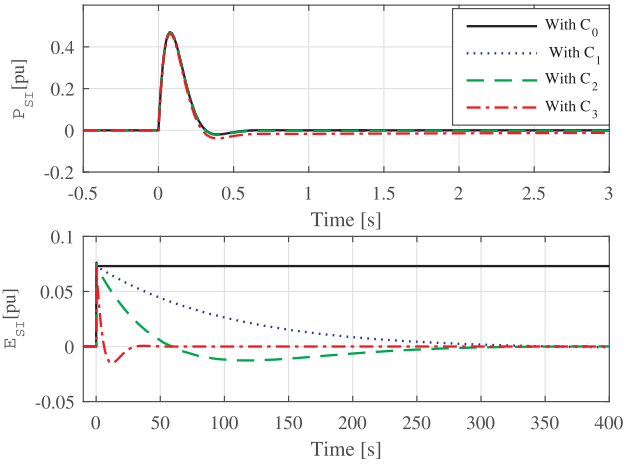

Fig. 3. Linear SI controller delivering inertia ($K_{d,SI} = 7.3, K_{p,SI} = 0$). Response to a −0.01 pu step in f, with varying speed of the energy recovery feedback loop, C_0–C_3. N.B: Different time scales in the two subplots.

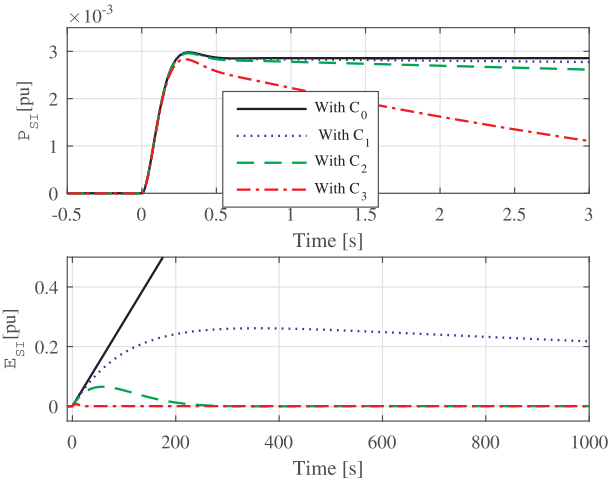

Fig. 4. Linear SI controller delivering damping ($K_{d,SI} = 0, K_{p,SI} = 0.29$). Response to a −0.01 pu step in f, with varying speed of the energy recovery feedback loop, C_0–C_3. N.B: Different time scales in the two subplots.

measure of the impact on the fatigue of the turbine, since it is related to cycling of the load on the guide vanes and, in the case of a Kaplan turbine, the runner blades [31,32].

3. Performance of a future system with low inertia and damping

This section describes how the grid frequency quality and the control work of the hydropower units providing FCR to the system are affected when the inertia and/or damping of the system are reduced by half. These results are also valid if the lost inertia is replaced by a synthetic inertia that is only activated when there is a major frequency event, as in the Hydro-Québec emulated inertia specification [3], since such an SI will not give any support in normal operation.

If the non-linearities (backlash in the hydropower regulating mechanism) are omitted, the system behaviour can be studied in frequency domain. Fig. 5 shows the gain of the closed loop transfer function from load disturbance, ΔP_L, to grid frequency, f, and to hydropower regulation, Y. Reduced system inertia increases the fast frequency deviations and also the fast regulations of hydropower, while reduced system damping increases the frequency deviations and hydropower regulations that have a period around 60 s.

The same changes are studied by time domain simulation of the system, including backlash in the hydropower regulating mechanism. A

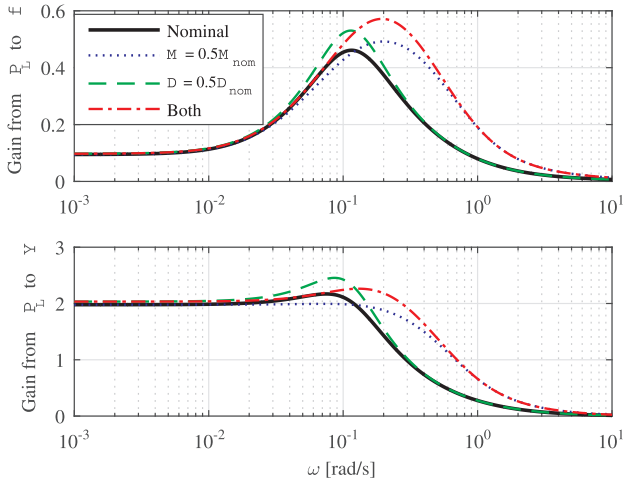

Fig. 5. System with half the inertia and/or damping (without SI) compared to the nominal system, in frequency domain. Gain from load disturbance ΔP_L to frequency deviation, f, and to hydropower guide vane opening deviation, ΔY.

Table 3
System performance of the nominal system compared to a system where the inertia and/or damping is reduced by half.

System	f_{rmse} [mHz]	Y_{dist} [%/h]	Y_{cycles} [#/h]
Nominal	56	32	38
$M = 0.5M_{nom}$	56	36	54
$D = 0.5D_{nom}$	58	37	41
Both	58	43	62

one week load disturbance time series calculated from grid frequency measurements [10] in February 2014 is used as input signal. The results are summarized in Table 3. The increased high frequency content of the grid frequency for low system inertia, that was visible in the Bode diagram in Fig. 5 is not visible as any increase in the f_{rmse}. However, low inertia increases the control work, especially Y_{cycles}, of the typical hydropower unit. Reduced damping has a stronger impact on f_{rmse} and Y_{dist}, but less impact on Y_{cycles}. When both the inertia and damping are halved, the control work increases with more than a third.

4. Replacing inertia and damping with synthetic inertia and damping

So, decreasing inertia and damping leads to increased control work in normal operation for units delivering FCR. Can a continuously active synthetic inertia and damping provided by the suggested linear SI-controller in Fig. 2 reduce this control work? If the SI-controller has access to an unlimited energy supply, so that the energy recovery parameter setting C_0 can be used, the answer is yes, as can be seen in Fig. 6. Here, the lost inertia is replaced by $K_{d,SI} = 7.3$ in the SI-controller, the lost damping is replaced by $K_{p,SI} = 0.285$, and the Bode gain curves end up on top of each other. The maximal difference between the curves occurs at 3 rad/s and is caused by the input signal filter, but the difference is too small to be visible in Fig. 6. Time domain simulation of the system including non-linearities gives the same performance in terms of f_{rmse},Y_{dist} and Y_{cycles} as the nominal system. A small part of the time domain signals are plotted in Fig. 7. With SI, the variations in the system frequency and the hydropower guide vane opening are reduced.

5. Synthetic inertia and damping with limited energy reserves

In most practical applications of SI, the power and energy available behind the SI-controller will be limited. Wind power needs to return to its optimal rotational speed and batteries need to stay partially charged.

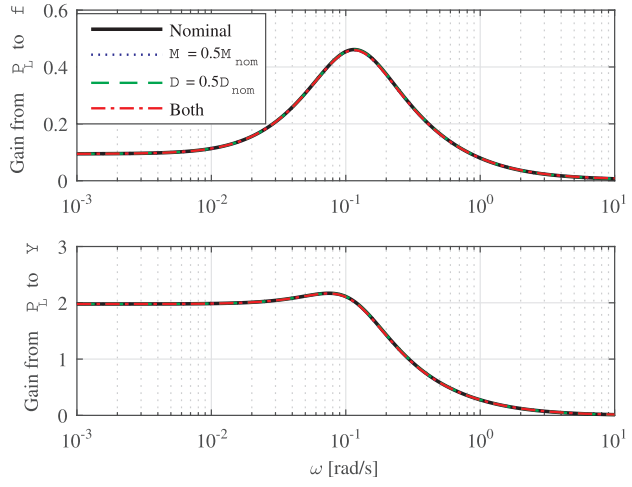

Fig. 6. System with half the system inertia and/or damping replaced by SI with unlimited energy reserve, in frequency domain. The system behaviour is the same as the nominal system (the curves are on top of each other).

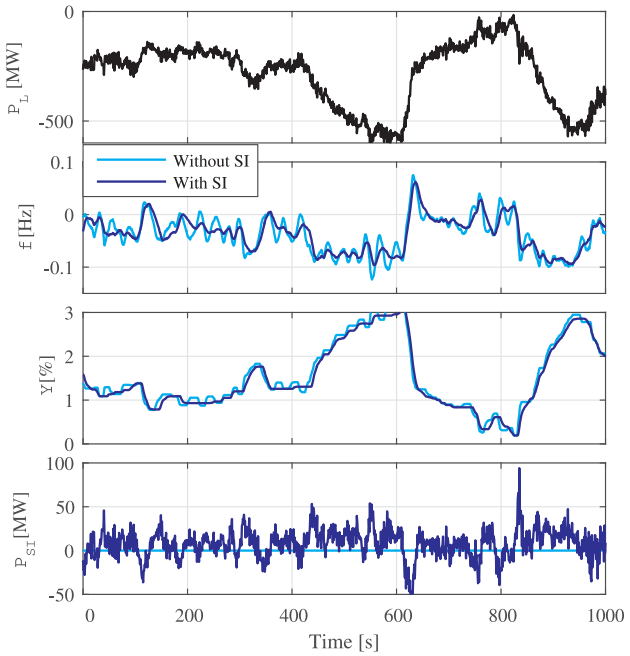

Fig. 7. System with $M = 0.5M_{nom}$ and $D = 0.5D_{nom}$, with and without SI with $K_{p,SI} = 0.29$ and $K_{d,SI} = 7.3$, in time domain. ΔP_L is the input signal.

In the model, a decrease in the production is equivalent to an increase in load and vice versa, since only the deviations from the scheduled point of operation are considered here. One way to avoid depletion of the energy reserve is to use an energy recovery scheme. With the energy recovery scheme suggested in Section 2.2, the recovery is smooth, and its speed can be adjusted, as exemplified by the settings C_0–C_3. The power and energy needed to provide SI will depend both on the controller setting C_0–C_3 and on the typical grid frequency variations of the system. If the amount of SI in the system is considerable, the SI will in turn impact the grid frequency. To quantify the power and energy required by the SI-controller, it is therefore better to simulate the whole system including SI and FCR, using a time series of typical load disturbances as input signal, than to simulate only the SI controller with the grid frequency as input signal.

The system performance with SI with setting C_0–C_3 is presented in Table 4, where replacement of inertia, damping and both inertia and damping with SI are presented separately. The results are from domain simulation including non-linearities with the same input data as in Table 3. Here, the relative change with respect to the performance of the nominal system (Table 3) is given. In all cases, SI with an infinite energy reserve (using C_0) can *maintain the nominal performance* of the system. However, the performance is worsened as the speed of the energy recovery is increased. The settings C_1 and C_2 still improves the system performance compared to the system without SI, but with the fastest energy recovery (C_3) the performance is worse than without SI.

Table 4
Relative change of the system performance when inertia and/or damping is replaced by energy limited SI, in percent of the values for the nominal system given in Table 3.

Case	f_{rmse} [mHz]	Y_{dist} [%/h]	Y_{cycles} [#/h]
Replacing M			
No SI	0%	14%	42%
C_0	0%	0%	0%
C_1	0%	3%	2%
C_2	1%	10%	7%
C_3	3%	69%	89%
Replacing D			
No SI	4%	16%	8%
C_0	0%	0%	0%
C_1	3%	1%	−1%
C_2	3%	3%	−2%
C_3	4%	17%	7%
Replacing M,D			
No SI	4%	37%	61%
C_0	0%	0%	0%
C_1	3%	4%	1%
C_2	4%	13%	5%
C_3	9%	110%	97%

The behaviour of the system with SI can be studied in frequency domain if the non-linearities are omitted. Figs. 8 and 9 show the gain of the closed loop transfer functions from P_L to f,Y,P_{SI} and E_{SI}. The main function of SI providing inertia can be seen as the decrease in high frequency gain from P_L to f and Y in Fig. 8. The energy recovery feedback loop of the SI controller makes the gain from P_L to E_{SI} go to zero at low frequencies. If the recovery is too fast (C_3), a peak appears in all the four transfer functions. In other words, the system becomes oscillatory, and this is reflected in the bad performance seen in Table 4. When the SI controller provides damping (Fig. 9) no such peak is formed, but the performance with C_3 approaches the performance without SI. The E_{SI} goes to infinity in the low frequency limit with C_0, but goes to zero with C_1–C_3 (although slowly with C_1).

Table 5 presents the power and energy output from the SI controller with C_0–C_3. The results are from the same simulation as the values in Table 4. The presented P_{req} and E_{req} are the values that are needed to cover the output of power and energy (peak to peak) of this period with a probability of 95%, i.e.

$$Pr(|P_{SI}| \leqslant P_{req}) = 95\% \tag{9}$$

$$Pr(E_{SI} \leqslant E_{max}) = 97.5\%, \quad Pr(E_{SI} \geqslant E_{min}) = 97.5\%$$
$$E_{req} = E_{max} - E_{min}. \tag{10}$$

The required capacity of an energy storage system that should provide SI is then $\pm P_{req}$ MW and E_{req} MWh, to cover the system need to a 95% probability. The values should be reasonably representative for the normal operation, but more data has to be analysed to get reliable extreme values. However, the maximal power need would correspond to approximately half the n − 1 disturbance of the system (since half of the inertia should be provided by SI and half by synchronous inertia).

The energy needed to provide SI in normal operation, E_{req}, is relatively small, as can be seen in Table 5. With C_0, the energy needed to provide damping is two orders of magnitude larger than the energy needed to provide inertia, but is still not unreasonable for modern battery systems. However, it must be kept in mind that E_{req} is highly dependent on the characteristics of the losses of the energy source, which are not included here. These values only correspond to the energy delivered to the grid.

6. Limit cycle analysis

As a complement to linear analysis and time domain simulations, the possible interaction of the backlash non-linearity in the hydropower guide vane regulating mechanism and the SI-controller can be studied by the method of describing functions [33]. The describing function, Y_f, of a backlash is

$$ReY_f(C) = \frac{1}{\pi}\left(\frac{\pi}{2} + \arcsin\left(1-\frac{2B_Y}{C}\right) + 2\left(1-\frac{2B_Y}{C}\right)\sqrt{\frac{B_Y}{C}\left(1-\frac{B_Y}{C}\right)}\right) \tag{11}$$

$$ImY_f(C) = -\frac{4B_Y}{\pi C}\left(1-\frac{B_Y}{C}\right), \tag{12}$$

where C is the amplitude of the limit cycle oscillation.

The Nyquist curve of the linear system is plotted in Fig. 10 together with the negative inverse of the describing function of the backlash, $-1/Y_f(C)$. If the Nyquist curve crosses the curve of the describing function, the system may be subject to limit cycle oscillations. This is

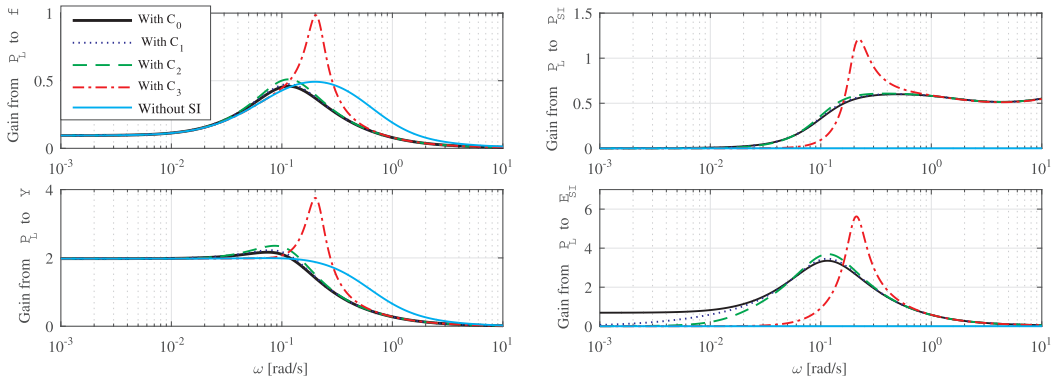

Fig. 8. System with half the system *inertia* replaced by SI with setting C_0–C_3 compared to the system without SI in frequency domain. Gain from load disturbance ΔP_L to grid frequency deviation Δf, guide vane opening deviation ΔY, SI power output P_{SI} and SI energy output E_{SI}.

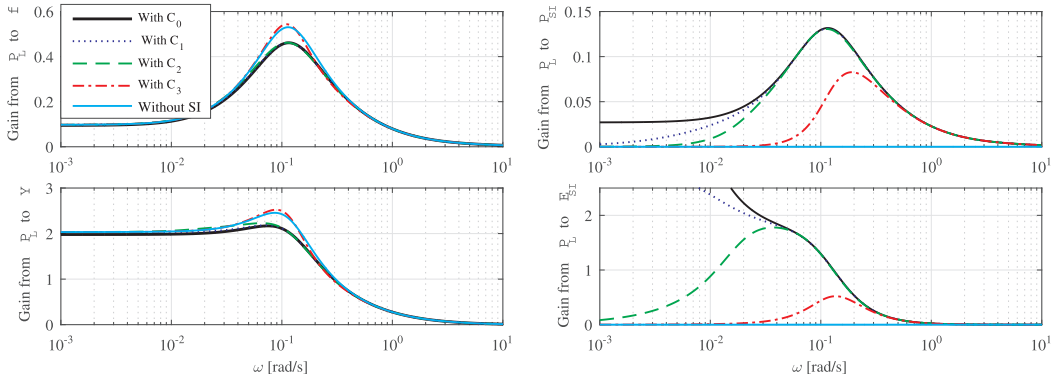

Fig. 9. System with half the system *damping* replaced by SI with setting C_0–C_3 compared to the system without SI in frequency domain. Gain from load disturbance ΔP_L to grid frequency deviation Δf, guide vane opening deviation ΔY, SI power output P_{SI} and SI energy output E_{SI}.

the case for the system with C_3. The stability margin of the system can be seen from the distance between the point $(-1, j0)$ and the Nyquist curve. It is clear that the stability margin is improved with SI with C_0 compared to the system without SI, but also that the stability margin is decreased with C_3.

7. Response to n − 1 disturbance

An n − 1 disturbance, which in the Nordic system is the loss of 1400 MW production, is simulated in Fig. 11. The nadir of the grid frequency is lower than in reality, because the disturbance reserve, FCR-D, which is activated when $f < 49.9$ Hz is not included in the model, but the relative impact from SI with C_0–C_3 can still be studied. All the SI-controllers decrease the ROCOF of the system, but the nadir is worsened with C_3. The oscillations of the system with C_3 die out after a few periods if the linear model is used to simulate the system, but turns into stable limit cycle oscillations if the non-linearities are included.

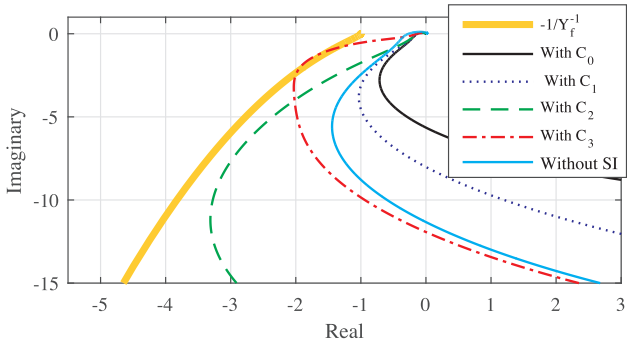

Fig. 10. The negative inverse of the describing function of a backlash and the Nyquist curves of the system with half the inertia and damping replaced by SI with C_0–C_3. A Nyquist curve that crosses the describing function curve indicates the possible existence of a limit cycle oscillation in the system.

8. Discussion

The energy and power needed to provide the suggested linear SI are moderate. There are already commercial projects installing batteries of a sufficient size for other ancillary services. For example, a battery park with a capacity of 22 MW and 15 MWh is presently being commissioned

Table 5
Power and energy need (P_{req} and E_{req}) of the SI controller in different scenarios, with C_0–C_3.

Scenario	$M = 0.5M_{nom}$		$D = 0.5D_{nom}$		*Both*	
	P_{req} (MW)	E_{req} (MWh)	P_{req} (MW)	E_{req} (MWh)	P_{req} (MW)	E_{req} (MWh)
C_0	24	0.32	23	92	34	92
C_1	25	0.11	7.9	0.94	26	0.95
C_2	25	0.11	7.5	0.09	27	0.14
C_3	32	0.079	2.6	0.012	34	0.092

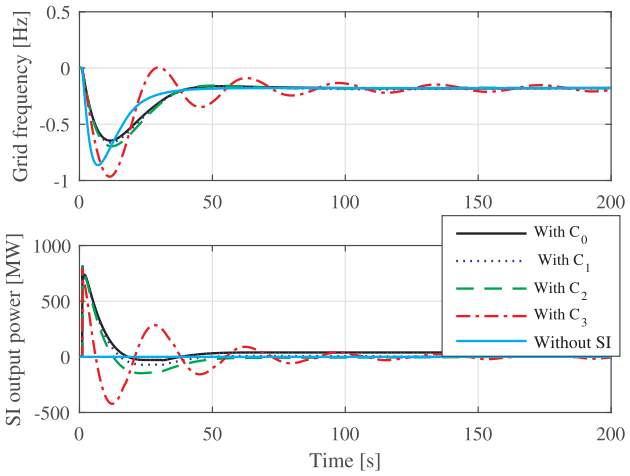

Fig. 11. Closed loop non-linear system response to a sudden loss of 1400 MW production. The system inertia and damping are half of the nominal values, but replaced by SI with varying energy recovery speed. The frequency nadir is lower than in reality, since the fast disturbance reserve, FCR-D, is not included in the model.

in Great Britain to provide frequency control reserves. That capacity is of the same order of magnitude as the needs of the Nordic system described in this paper.

Damping provided by the suggested linear SI may also be efficient in damping of inter-area oscillations. Synthetic damping has been shown to be able to damp electro-mechanical oscillations in previous research [11]. The basic property, to create an output power that is proportional to the grid frequency deviation, is also used in power system stabilizers (PSSs) to damp inter-area oscillations.

The dynamic properties of the specific device controlled by the SI controller will have a small influence on the results. To check the sensitivity to dynamics in the 0.1–1 Hz band, the system was simulated with 5 and 10 times as large low pass filter time constant (T_f). This changed the results with only a few percent.

It should be mentioned that there are other possibilities in how to tune the SI energy recovery feedback loop than the one suggested in this paper. If a more oscillatory behaviour from the SI recovery is accepted, i.e. $\|S(i\omega)\|_\infty > 1$, the gain from ΔP_L to f can be improved even with shorter recovery time. However, such a tuning is worse from a limit cycle oscillation perspective, because it leads to larger phase shift which pushes the Nyquist curve further to the left in the third quadrant, and past the describing function curve. Taking this into consideration, $\|S(i\omega)\|_\infty \leqslant 1$ seems like a good requirement for the SI controller.

9. Conclusion

This paper suggests a new, linear and continuously active SI controller that could be used to replace the inertia and damping lost from the system when conventional synchronous generators are replaced by inverter connected VRE. Contrary to the disturbance reserve SI specified by e.g. Hydro Québec and EirGrid, the suggested linear SI can support the grid both when there is a large disturbance *and* in normal operation. If the lost inertia is not replaced, or is replaced by disturbance reserve SI, the frequency deviations during normal operation will increase and the wear and tear of hydropower and other units providing frequency control to the system will increase. This leads to worse margins for large disturbances, since the grid frequency may already be low when a large unit is disconnected, and is likely to increase the costs for frequency control reserves. If the lost inertia is replaced by the suggested linear SI, these consequences can be avoided. It would also be possible to improve the system performance by employing even more inertia and damping from linear SI controllers. However, great care must be taken to make sure that energy recovery schemes in SI-controllers do not in practice eliminate the benefit for the grid and for the FCR units. Apart from the linear aspects, the energy recovery schemes in SI-controllers may also cause limit cycle oscillations in the regulating mechanisms of FCR units, if inappropriately parametrized.

Acknowledgment

The research presented was carried out as a part of “Swedish Hydropower Centre – SVC” and “StandUp for Energy”. SVC has been established by the Swedish Energy Agency, Elforsk and Svenska Kraftnät together with Luleå University of Technology, The Royal Institute of Technology, Chalmers University of Technology and Uppsala University. www.svc.nu.

References

[1] Kovaltchouk T, Debusschere V, Bacha S, Fiacchini M, Alamir M. Assessment of the impact of frequency containment control and synthetic inertia on intermittent energies generators integration. In: 2016 Eleventh international conference on ecological vehicles and renewable energies (EVER); 2016. http://dx.doi.org/10.1109/EVER.2016.7476361.

[2] Díaz-González F, Hau M, Sumper A, Gomis-Bellmunt O. Participation of wind power plants in system frequency control: review of grid code requirements and control methods. Renew Sustain Energy Rev 2014;34:551–64.

[3] Brisebois J, Aubut N. Wind farm inertia emulation to fulfill Hydro-Québec’s specific need. In: 2011 IEEE power and energy society general meeting; 2011. http://dx.doi.org/10.1109/PES.2011.6039121.

[4] Ruttledge L, Flynn D. System-wide inertial response from fixed speed and variable speed wind turbines. In: 2011 IEEE power and energy society general meeting; 2011. http://dx.doi.org/10.1109/PES.2011.6038883.

[5] Vogler-Finck PJ, Fruh W-G. Evolution of primary frequency control requirements in great britain with increasing wind generation. Int J Electr Power Energy Syst 2015;73:377–88. http://dx.doi.org/10.1016/j.ijepes.2015.04.012.

[6] Miller NW, Clark K, Shao M. Frequency responsive wind plant controls: impacts on grid performance. In: 2011 IEEE power and energy society general meeting; 2011. http://dx.doi.org/10.1109/PES.2011.6039137.

[7] Fischer M, Engelken S, Mihov N, Mendonca A. Operational experiences with inertial response provided by type 4 wind turbines. IET Renew Power Gener 2016;10(1):17–24. http://dx.doi.org/10.1049/iet-rpg.2015.0137.

[8] Saarinen L, Norrlund P, Lundin U. Tuning primary frequency controllers using robust control theory in a power system dominated by hydropower. In: Proceedings of the CIGRÉ session 2016; 2016.

[9] Yang W, Norrlund P, Saarinen L, Yang J, Guo W, Zeng W. Wear and tear on hydro power turbines – influence from primary frequency control. Renew Energy 2016;87(Part 1):88–95.

[10] Yang W, Norrlund P, Saarinen L, Yang J, Zeng W, Lundin U. Wear reduction for hydropower turbines considering frequency quality of power systems: a study on controller filters. IEEE Trans Power Systems. http://dx.doi.org/10.1109/TPWRS.2016.2590504.

[11] Gautam D, Goel L, Ayyanar R, Vittal V, Harbour T. Control strategy to mitigate the impact of reduced inertia due to doubly fed induction generators on large power systems. IEEE Trans Power Syst 2011;26(1):214–24. http://dx.doi.org/10.1109/TPWRS.2010.2051690.

[12] Singh M, Allen AJ, Muljadi E, Gevorgian V, Zhang Y, Santoso S. Interarea oscillation damping controls for wind power plants. IEEE Trans Sustain Energy 2015;6(3):967–75. http://dx.doi.org/10.1109/TSTE.2014.2348491.

[13] Torres MA, Lopes LAC, Morán LA, Espinoza JR. Self-tuning virtual synchronous machine: a control strategy for energy storage systems to support dynamic frequency control. IEEE Trans Energy Convers 2014;29(4):833–40. http://dx.doi.org/10.1109/TEC.2014.2362577.

[14] Alipoor J, Miura Y, Ise T. Power system stabilization using virtual synchronous generator with alternating moment of inertia. IEEE J Emerg Sel Top Power Electron 2015;3(2):451–8. http://dx.doi.org/10.1109/JESTPE.2014.2362530.

[15] Liu J, Miura Y, Ise T. Comparison of dynamic characteristics between virtual synchronous generator and droop control in inverter-based distributed generators. IEEE Trans Power Electron 2016;31(5):3600–11.

[16] Serban I, Ion CP. Microgrid control based on a grid-forming inverter operating as virtual synchronous generator with enhanced dynamic response capability. Int J Electr Power Energy Syst 2017;89:94–105. http://dx.doi.org/10.1016/j.ijepes.2017.01.009.

[17] Zhong QC, Konstantopoulos GC, Ren B, Krstic M. Improved synchronverters with bounded frequency and voltage for smart grid integration. IEEE Trans Smart Grid. http://dx.doi.org/10.1109/TSG.2016.2565663.

[18] Ullah NR, Thiringer T, Karlsson D. Temporary primary frequency control support by variable speed wind turbines – potential and applications. IEEE Trans Power Syst 2008;23(2):601–12. http://dx.doi.org/10.1109/TPWRS.2008.920076.

[19] Wang-Hansen M, Josefsson R, Mehmedovic H. Frequency controlling wind power modeling of control strategies. IEEE Trans Sustain Energy 2013;4(4):954–9. http://dx.doi.org/10.1109/TSTE.2013.2257898.

[20] Wu L, Infield DG. Towards an assessment of power system frequency support from wind plant; modeling aggregate inertial response. IEEE Trans Power Syst

2013;28(3):2283–91. http://dx.doi.org/10.1109/TPWRS.2012.2236365.
[21] Wang Y, Delille G, Bayem H, Guillaud X, Francois B. High wind power penetration in isolated power systems – assessment of wind inertial and primary frequency responses. IEEE Trans Power Syst 2013;28(3):2412–20.
[22] Miao L, Wen J, Xie H, Yue C, Lee WJ. Coordinated control strategy of wind turbine generator and energy storage equipment for frequency support. IEEE Trans Ind Appl 2015;51(4):2732–42. http://dx.doi.org/10.1109/TIA.2015.2394435.
[23] França BW, de Castro AR, Aredes M. Wind and photovoltaic power generation integrated to power grid through DC link and synchronverter. In: 2015 IEEE 13th Brazilian power electronics conference and 1st southern power electronics conference (COBEP/SPEC); 2015. http://dx.doi.org/10.1109/COBEP.2015.7420216.
[24] Arani MFM, El-Saadany EF. Implementing virtual inertia in DFIG-based wind power generation. IEEE Trans Power Syst 2013;28(2):1373–84. http://dx.doi.org/10.1109/TPWRS.2012.2207972.
[25] Chang-Chien LR, Lin WT, Yin YC. Enhancing frequency response control by DFIGs in the high wind penetrated power systems. IEEE Trans Power Syst 2011;26(2):710–8. http://dx.doi.org/10.1109/TPWRS.2010.2052402.
[26] Ørum E, Kuivaniemi M, Laasonen M, Bruseth AI, Jansson EA, Danell A, et al. Future system inertia. Tech rep. Enstso-e; 2015.
[27] Saarinen L, Norrlund P, Lundin U, Agneholm E, Westberg A. Full-scale test and modelling of the frequency control dynamics of the Nordic power system. In: 2016 IEEE power and energy society general meeting; 2016. http://dx.doi.org/10.1109/PESGM.2016.7741711.
[28] Saarinen L, Norrlund P, Lundin U. Field measurements and system identification of three frequency controlling hydropower plants. IEEE Trans Energy Convers 2015;30(3):1061–8. http://dx.doi.org/10.1109/TEC.2015.2425915.
[29] Segovia VR, Hägglund T, Åström K. Measurement noise filtering for common PID tuning rules. Control Eng Pract 2014;32:43–63.
[30] Lindsjö H, Wurm E, Leponen M. Design aspects of oil-free Kaplan runners. Int J Hydropower Dams 2015;22(4):78–83.
[31] Wurm E. Consequences of primary control to the residual service life of Kaplan runners. In: Russia power 2013 and hydrovision Russia 2013, Moscow, Russia; 2013.
[32] Storli P-T, Nielsen TK. Dynamic load on a Francis turbine runner from simulations based on measurements. In: IOP conference series: earth and environmental science; 2013, vol. 22, no. 3. Article no. 032056.
[33] Glad T, Ljung L. Control theory: multivariable and nonlinear methods. 2nd ed. Taylor & Francis; 2000.